© Filodiritto Editore – Proceedings

Identifying the Annual Signal in Laminated *Lingula* Shales of Middle Permian Age

CHERNOVA Inna[1], NOURGALIEV Danis[1], VAFINA Gulnur[1], CHERNOVA Olga[1]

[1] *Kazan Federal University (RUSSIA)*
Email: inna.chernova@kpfu.ru

Abstract

This paper describes methods for identifying annual laminations in Middle Permian shales.

Laminations were studied by analyzing scans of polished samples of shale. Spectral analysis of couplets showed harmonic elements with periods that are multiples of 11, indicating the seasonal nature of lamination and providing an opportunity for determining the sedimentation rate.

The sedimentation rate is estimated at 0.15 mm per year and differs significantly from estimates obtained earlier. Perhaps not all couplets should be considered annual. The question of which layers should be considered as annual and which should not, remains open, and requires further study.

Keywords: annual laminations, depositional cycle, thin-laminated shales, Late Permian, image processing

Introduction

Annual (or seasonal) layering – a special type of periodic layering – is characteristic of many fine-grained rocks. The best known of these are varves, i.e. layers of lake sediments with contrasting color, mineral composition and organic content. The interest in varved lake sediments has increased, because of their potential as records for studying environmental and climate variability at a precise and high-resolution time-scale [1], [2], [3], [4], [5], [6], [7]. Annual values of minerogenic and organic matter accumulation rates can reveal specific information about variability of past processes, and their relationship to changing climate. Studies of climate variations using modern lake sediments are commonly limited to the Holocene. However, climate changes have also occurred much earlier, and little is known about those changes.

In the meantime, thin-layered rocks older than Holocene age are very common, and their study appears reasonable and justified. For example, if one knows the time interval during which the ancient sediments were accumulated, one can use it in a paleomagnetic study to determine the periods of geomagnetic variations [8], [9]. Correlations between global climate change and geomagnetic reversals, in turn, provide important information that assists with development of science and scientific knowledge about the evolution of the Earth's core and mantle [10], [11].

For this project, thin-layered rocks of Middle Permian age known as *Lingula* Shale Member (Lower Kazanian Substage) were studied. This paper discusses the nature of layers in *Lingula* Shale Member and addresses the methods that can be used to determine the thickness of contrasting layers and identify different sedimentation cycles.

Study site and materials

The samples from *Lingula* Shale Member were taken from the outcrop along the right bank of the Kama River, near the mouth of the Tanaika River (55°44'N, 51°51'E, Tatarstan, Russia) (Fig. 1a, b).

The sediments are of Middle Permian (P_2) age. They are thin-layered green-gray calciferous shales with reddish-brown and yellow interlayers and can be found in the Ufimian (uppermost Kungurian of the International Chronostratigraphic Chart) – Kazanian boundary beds. X-ray diffraction analysis and chemical analysis showed that light layers are composed of carbonates (primarily calcite). Dark

layers consist of shale minerals containing organic material. Brown layers are made up of sediments enriched with iron oxides and hydroxides (that explains the color). The term "*Lingula* Shale Member" refers to the brachiopod *Lingula orientalis* Gol., the remains of which are often found in these rocks.

As an experiment, the sample with the most distinct layering was selected, and an image of its polished surface was analyzed (Fig. 1c). To obtain the image, the sample was placed into a scanner.

Scanning resolution was 1200 dpi (the rest of the settings were left at their defaults, because they did not affect the image quality).

Visually, several layer types can be observed (Fig. 1e):

- light (almost white) layers about 1 mm thick, usually not even, thinning lengthwise;
- light layers about 0.1 mm thick (some of them are bright and easily traced along the entire sample, others are hardly noticeable);
- dark layers 0.1-3 mm thick;
- brownish-yellow and red layers, combining several light and dark interlayers.

The thickest light layers were on further examination found to be inhomogeneous, formed by sequencing white layers 0.07 mm thick, and much thinner dark layers.

Methodology

The task of determining the nature of varves was, initially, solved as a more focused problem of distinguishing couplets, determining their number, and measuring the thickness of each couplet.

There are several image processing applications (including freely distributed ones) that can be of use: MultiSpec, ImageJ, Scion Image, etc. Many of them are widely used in biology and medicine.

There are also commercial software products (such as DendroScan) developed for measuring tree-ring width and density. Cybis Coordinate Recorder and BMPix and PEAK tools [12] are also often used in image analysis and estimation of varve thickness. Some of these software products can be tailored to our needs. However, the images used in this project are much more complex than the images of annual tree-rings or varves. Therefore, their processing requires a larger tool set.

ERDAS Imagine has tremendous capabilities for useful-signal isolation, raster compression and display, so it was used to process the images of the shale samples and layer thickness evaluation.

Filtering

Since shale is a soft material, it is impossible to obtain a perfectly flat mirror-like surface when grinding and polishing it.

There are always some scratches and imperfections that produce spots and lines on the final image.

Uneven scanner lighting also affects image quality.

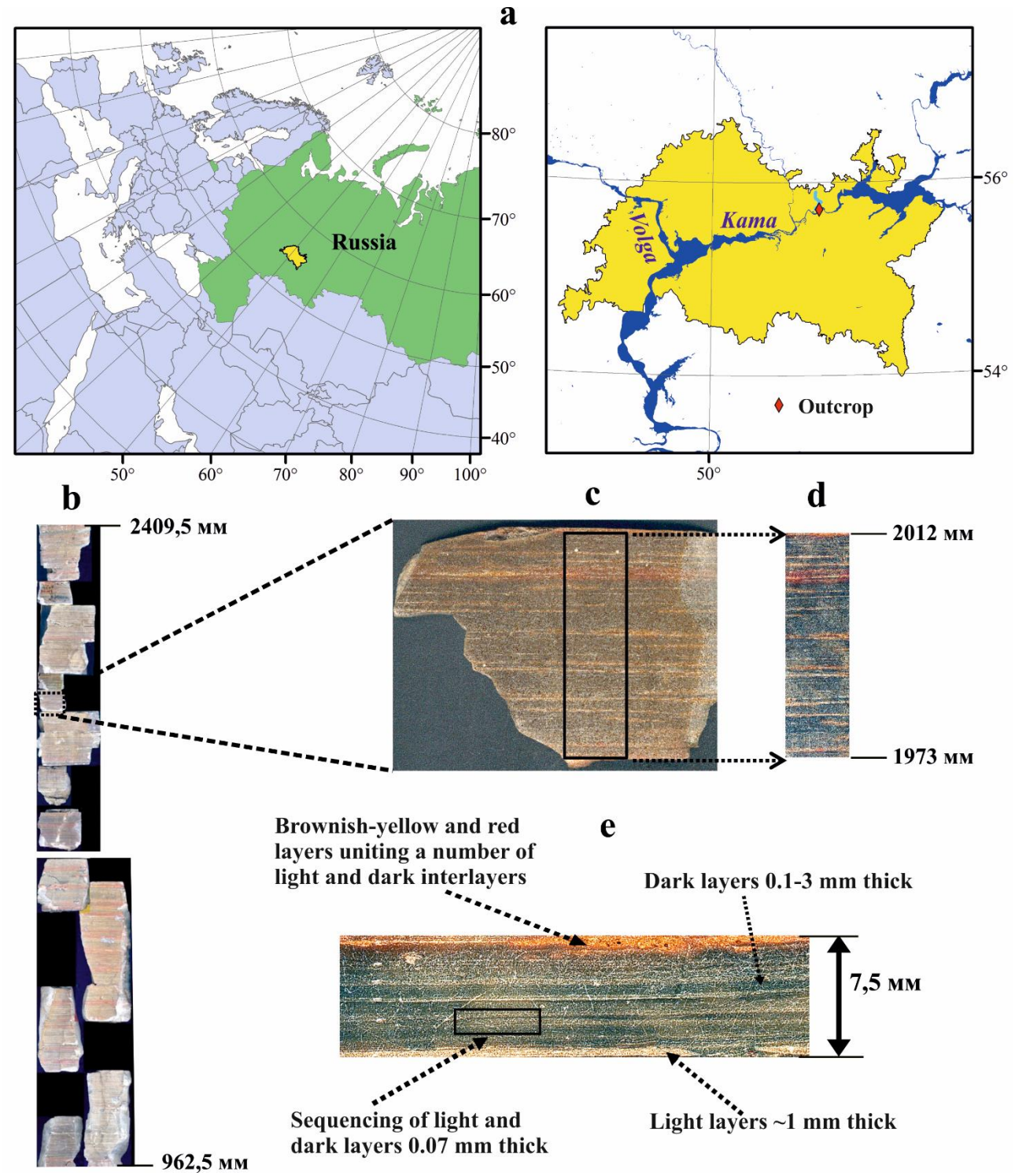

Fig. 1. Study site and materials: (a) study area, (b) studied section part, (c) studied sample, (d) noise free fragment cut from the original scan, (e) detailed description of layers.

It is impossible to filter high-level noise like cracks, spots or wide strips on the image without losing useful information. Therefore, such areas are not included in the analysis. So, a noise free fragment was cut from the original image and further analyzed (Fig. 1d). All further filtering and image analysis operations were performed using this fragment only.

A grinding wheel always leaves slight scratches on the sample's surface. On the image, they appear in the form of circular chaotically oriented lines, which can, however, be filtered out. ERDAS Imagine has many tools for image quality enhancement [13]. Of all filtering methods, Fourier transformation is best suited to our needs. Experiments with filters have shown that:

- a low-pass filter removes "ripples" appearing on the image due to surface imperfections;
- a rectangular filter enhances the contrast of layer edges;
- a high-pass filter adjusts the image contrast and emphasizes the boundaries of the light layers;
- a wedge filter removes noise in the form of subvertical stripes.

A well-chosen combined filter can significantly improve the original image (Fig. 2).

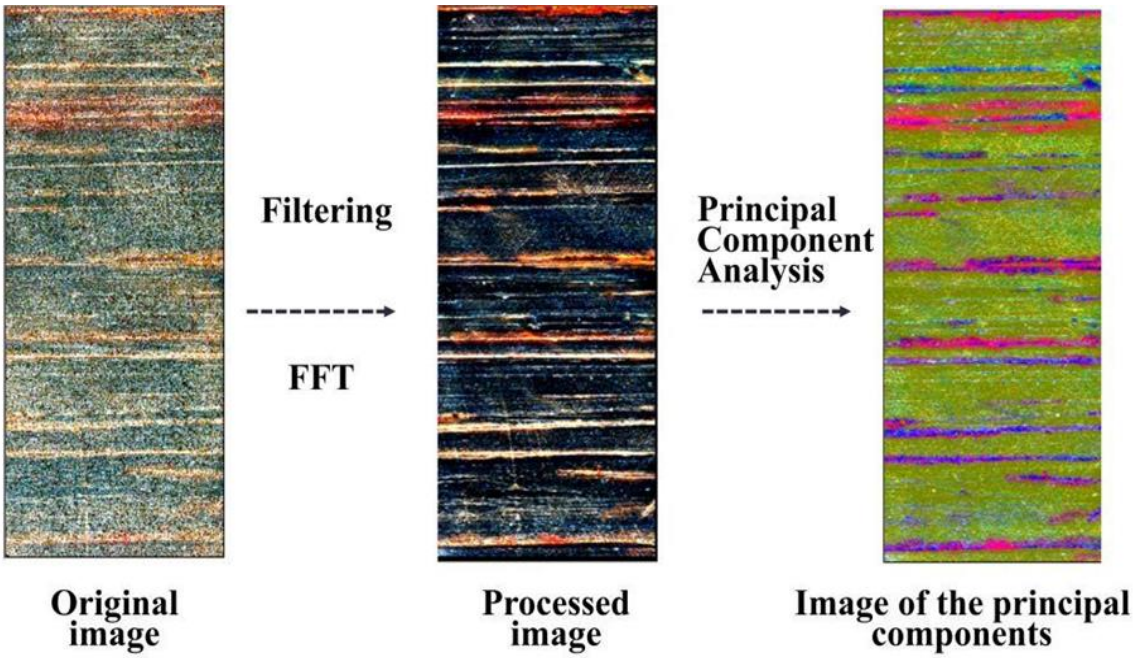

Fig. 2. Main stages of image processing.

Data compression

The next step of the image processing is principal component analysis (PCA). Prerequisites for the use of PCA are as follows. The scanned image is in RGB mode, and all three bands of the image contain the same information (this can be seen visually, simply comparing the bands of the image).

A high correlation coefficient (0.68-0.92) between the bands also indicates information redundancy.

Principal component analysis is a recognized data compression method [13] and has produced interesting results.

The image of the principal components is shown in (Fig. 2). It contains three bands displaying the values for the 1st, 2nd and 3rd components, respectively.

The most important are the two components with a total weight of 99.1% (Table 1). The influence of the third component on the values is not significant, so it was excluded from the analysis.

Table 1. Factor-variable correlations (factor loadings).

Factor-variable correlations (factor loadings)			
Variable	Factor 1	Factor 2	Factor 3
RED	0.59	-0.74	0.32
GREEN	0.61	0.14	-0.77
BLUE	0.52	0.65	0.54
% Total variance	88.6	10.5	0.9

Looking at the 1st component (Fig. 3), its meaning is obvious: the 1st principal component clearly shows the sequencing of light and dark layers, i.e. lamination.

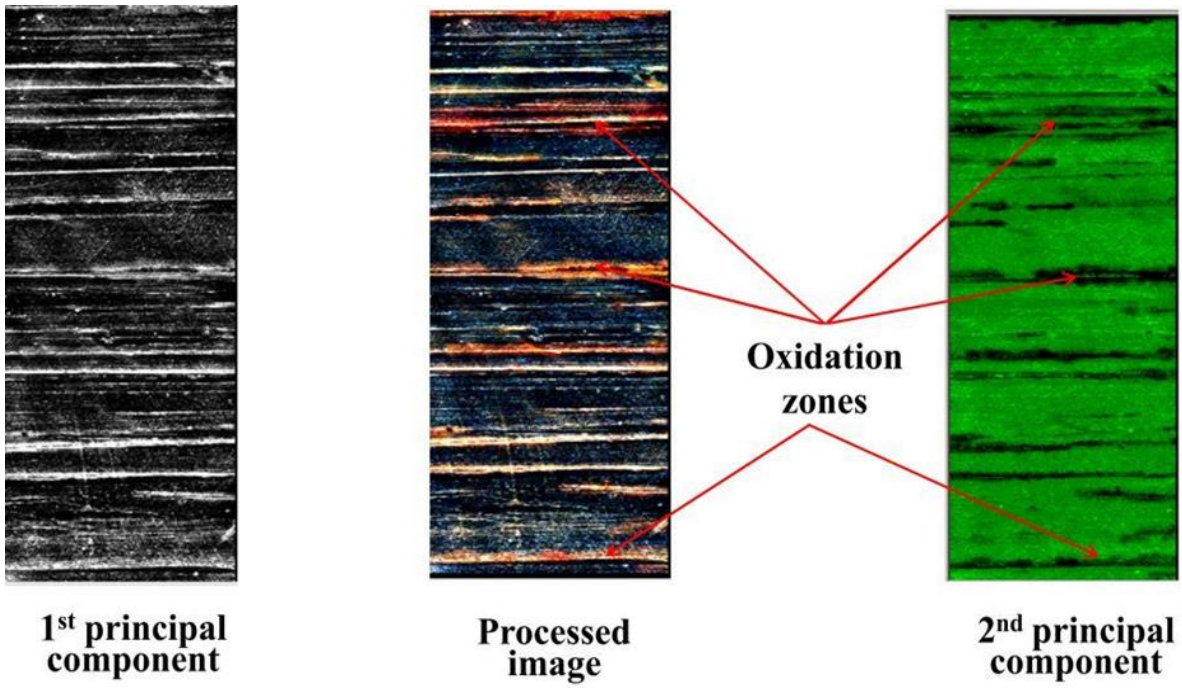

Fig. 3. Principal component analysis results.

The second principal component reliably correlates with the oxidation zones. This can be seen visually when comparing the images (Fig. 3): dark areas of the 2nd principal component corresponds to the areas of dominating red on the original image. This is also evidenced by the high factor loading (-0.74) of the 2nd component (Table 1).

The possibility of defining oxidation zones on the images may be also useful for further studies, since there is a perception that oxidation zone formation is a periodic process following an 11-year solar cycle [14].

Thickness of couplets

Returning to the first principal component: (Fig. 4) shows the distribution of pixel values along AB for the original image (on the left) and the first principal component (on the right). It is clear that the right graph is more differential and easier to read than the left one. Each spike corresponds to a light-colored layer. Therefore, it is quite easy to determine the number of light layers, their location, as well as to differentiate them by brightness (it should be noted here that this term does not imply spectral brightness; it is referred to the values of the first principal component on the basis of which the pixels were classified, so the word "brightness" is used for convenience, since the larger the value of the principal component, the more vivid a color the pixel obtains).

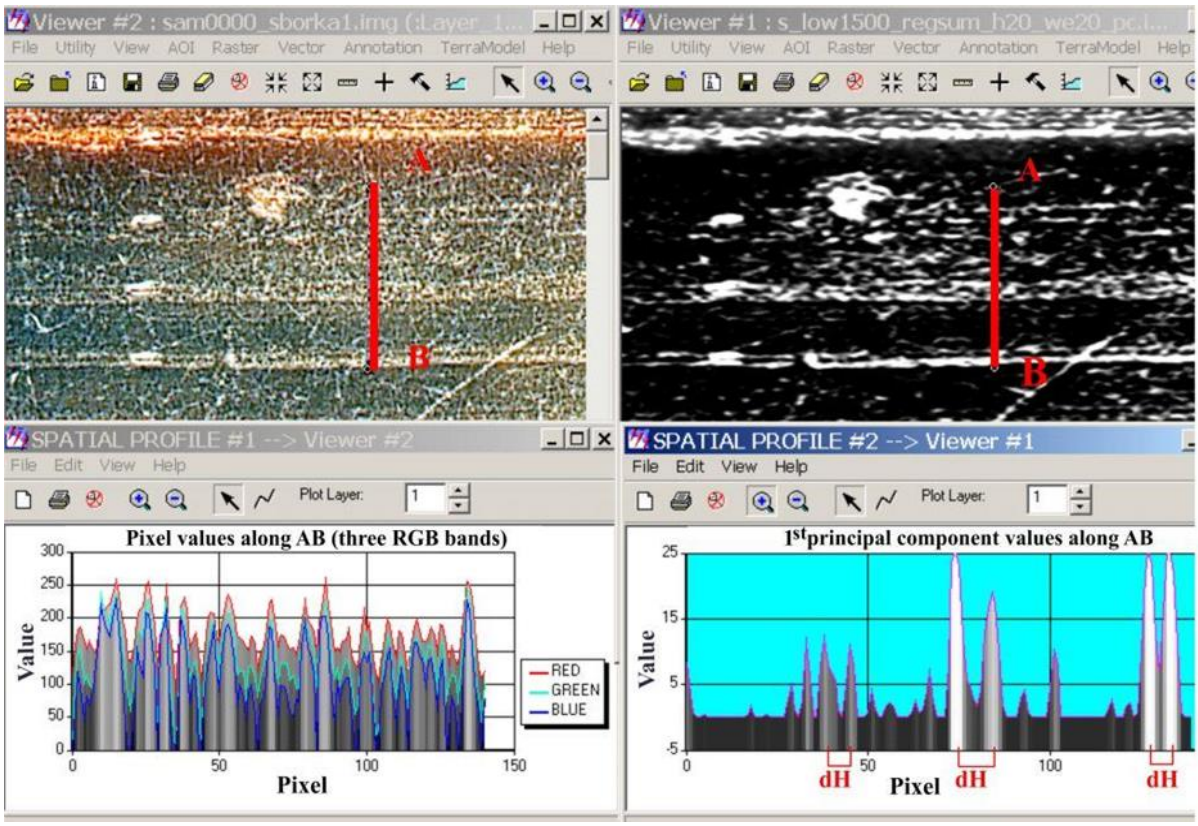

Fig. 4. Original (on the left) and processed images (on the right).

A detailed comparison of the original image and the 1st principal component showed that image processing cuts a very small number of light layers from the image. These are the layers with almost the same brightness as the dark ones.

Further calculations are simple mathematical procedures. Because the bedding is horizontal, each raster column can be used as an input to calculate the number of couplets and determine their total thickness: differences in the neighboring spikes' dH coordinates (Fig. 4) give the thickness of a couplet in pixels. In most cases, the layers are interrupted by gaps along their entire length (this happens because pixels representing the same layer can be bright in one place and dark in another despite their location – on the same horizontal line). Therefore, in order to cover all the layers, mean pixel values calculated for each row of the raster were used. Knowing the number of millimeters in a pixel enables one to determine the thickness of a couplet.

The results of the calculations are as follows: there are 453 couplets in a sample 7.2 cm thick. The average thickness of the couplet is 0.15 mm.

Results and discussions

The area in (Fig. 1a) was located at ≈20-30° latitude during the Late Permian, so the sedimentation process took place in a warm climate that had no winter [15]. We believe that in arid climates, lighter layers (chemogenic) formed during dry seasons, while darker ones (consisting of clay and organic material) accumulated during rainy seasons. Brown interlayers indicate that sometimes (maybe periodically) sedimentation took place under oxidizing conditions.

Assuming that a couplet of light and dark layers represents a seasonal cycle of sedimentation (driven by annual climate variations), the number of such couplets gives the number of years captured in the studied sequence. The laminations can be not only of a seasonal nature, but may also relate to local climate features, geomorphology and other factors. It is also possible that dry and rainy seasons repeated many times within a year, or rainy seasons occurred once every few years. Therefore, the problem of identifying the nature of lamination in the *Lingula* Shales still stands.

The seasonal nature of laminations, if proved, is sufficient for sedimentation rate evaluation.

The most common, simple and reliable way of proving it is finding a correlation between laminations and climatic changes or solar activity. A more feasible approach for varved records is to detect periodicities in time series that can be matched to well-known solar cycles, like the 11-year Schwabe, the 22-year Hale or the 80-90-year Gleisberg cycles) [9].

Solar cycles of ≈5.5 and ≈8.5 years are also well known. Undoubtedly, all these cycles are reflected in the sediments. In modern lake sediments, the following cycles were observed: 2.6-3.3 years, 5-5.9 years, 10.6-12.6 years. A detailed study of microlaminations in sedimentary rocks of various ages indicates that 11-year cycles are most vividly reflected in seasonal microlaminations. These cycles' duration in the Phanerozoic was quite constant: from ≈10 to ≈13 years. This is a fundamental feature in proving the seasonal nature of microlaminations. Periodical variations in the thickness of couplets (repeated every ≈10-13 couplets) indicates the seasonal nature of laminations and provides opportunities for determining the sedimentation rate. The calculations usually have a 15-20% margin of error, which is close to the required level for determining the periods of secular geomagnetic variations.

The maximum entropy method (MEM) [16] was used for spectral analysis of the couplet thickness.

In contrast to the Fourier, MEM is more suitable for identifying short-term cycles within small data sets. On the MEM spectrum (Fig. 5), in a high-frequency band, variations 0.15 mm per year, considering all the layers. Based on general ideas about the accumulation rates for such sediments, this value is very small, and it differs significantly from estimates obtained earlier [14]. Although the spectral analysis of the couplet thickness showed harmonics with periods that are multiples of 11, not all couplets should be considered annual.

Assuming that the layer brightness is an indicator of certain sedimentary environments, classification of the layers by their brightness can greatly help in the interpretation of results.

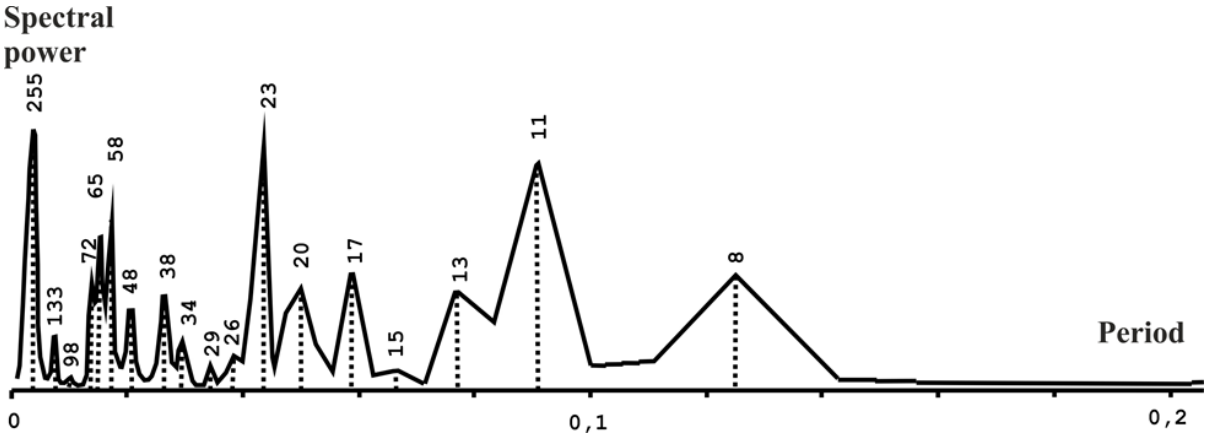

Fig. 5. Maximum entropy method spectrum.

The brightness values vary from 0 to 57. Dividing the entire range of values into equal intervals (0-10, 10-20, 20-30, 30-40, 40-50 and 50+) reveals that starting from the 20-30 interval the number of layers falling into each interval increases by 10 times. Selecting this interval as a threshold for classification allows the layers to be divided into 2 groups. The first group includes the brightest layers. They comprise ≈1/6 of all layers. The other group includes all the rest (their brightness is 2-5 times less than the brightness of the first group).

If the layers of the first group are considered to be seasonal ones, and the rest represent noise not related to seasonal climate variations, the estimate of sedimentation rate would be 1 mm per year, which is more believable.

Thus, the question of which layers should be considered annual and which should not, remains open and requires further study.

Conclusions

The proposed method for studying laminations produced satisfactory results and has a number of advantages:

1) two-dimensional Fourier filtering improves the original image significantly, which simplifies the recognition of microlaminations. Thus, the problem is solved without loss of useful information.
2) original image derivatives obtained using the principal component analysis showed that the sediment coloring depends on 2 factors: sediment composition and climatic conditions, which is quite obvious. However, the very fact that the sediment color can be divided into components relating to 2 types of laminations of different scales and natures is of scientific interest.

It is also clear that it is much harder to determine the nature of laminations in ancient sediments than to reveal seasonal layers in modern lake sediments. To reveal short-period paleoclimatic variations, detailed mineralogical, magnetic and isotope (oxygen and carbon) studies are needed.

Acknowledgments

The work was supported by the Ministry of Education and Science of the Russian Federation (project No. 02. G25.31.0170) and by the subsidy of the Russian Government to support the Program of Competitive Growth of Kazan Federal University among the World Leading Academic Centers.

REFERENCES

1. Dean, W. E., Bradbury, J. P., Anderson, R. Y., Barnosky, C. W. (1984). The variability of Holocene climate change – evidence from varved lake-sediments. Science 226, pp. 1191-1194.
2. Anderson, R. Y. (1992). Possible connection between surface winds, solar-activity and the Earth's magnetic-field. Nature 358, pp. 51-53.
3. Lotter, A. F., Sturm, M., Teranes, J. L., Wehrli, B. (1997). Varve formation since 1885 and high-resolution varve analyses in hypertrophic Baldeggersee (Switzerland). Aquatic Sciences 59, pp. 304-325.
4. Snowball, I., Zillén, L., Gaillard, M. J. (2002). Rapid early-Holocene environmental changes in northern Sweden based on studies of two varved lake-sediment sequences. Holocene 12, pp. 7-16.
5. Tiljander, M., Saarnisto, M., Ojala, A. K., Saarinen, T. (2003). A 3000-year palaeoenvironmental record from annually laminated sediment of Lake Korttajarvi, central Finland. Boreas 32, pp. 566-577.
6. Ojala, A. E. K., Alenius, T. (2005). 10000 years of interannual sedimentation recorded in the Lake Nautajarvi (Finland) clastic-organic varves. Palaeogeography Palaeoclimatology Palaeoecology 219, pp. 285-302.
7. Haltia-Hovi, E., Saarinen, T., Kukkonen, M. (2007). A 2000-year record of solar forcing on varved lake sediment in eastern Finland. Quaternary Science Reviews 26, pp. 678-689.
8. Nurgaliev, D., Borisov, A., Heller, F., Burov, B., Jasonov, P., Khasanov, D., Ibragimov, Sh. (1996). Geomagnetic secular variations through the last 3500 years as recorded by lake Aslikul sediments from Eastern Europe (Russia). Geophysical Research Letters 23, pp. 375-378.
9. Zolitschka, B., Francus, P., Ojala, A. E. K., Schimmelmann, A. (2015). Varves in lake sediments – a review. Quaternary Science Reviews 117, pp. 1-41.
10. Jacobs, J. A. (1987) The Earth's Core. 2nd Ed. International Geophysics Series, Volume 37. Academic Press, New York, London, 426.
11. Petrova, G. N. (1977). Geomagnetic data on the Earth's core. Izvestiya Akademii nauk SSSR. Fizika Zemli 11, pp. 9-11.
12. Weber, M. E., Reichelt, L., Kuhn, G., Pfeiffer, M., Korff, B., Thurow, J., Ricken, W., (2010). BMPix and PEAK tools: new methods for automated laminae recognition and counting – Application to glacial varves from Antarctic Marine sediment. Geochemistry, Geophysics, Geosystems 11 (1), 1-18.
13. ERDAS IMAGINE Tour Guides. (2006). Leica Geosystems Geospatial Imaging, LLC, 730.
14. Nourgaliev, D. K., Khasanov, D. I. (1992). Solar cycles recorded in Late Permian sediments. Solnechnye dannye 8, pp. 82-85.
15. Forsch, N. N. (1955). Volga-Ural Petroleum and Gas Province. Permian deposits. Ufimian sequence and Kazanian Stage. Trudy Vsesoyuznogo nauchno–issledovatelskogo Geologo-Razvedochnogo Instituta 92, pp. 1-156.
16. Andersen, V. 1974. On the calculation of filter coefficients for maximum entropy spectral analysis. Geophysics 39 (1), pp. 69-72.